Drying and Rehydration Kinetics of Mangoes: Solute Effects

Maldonado, Silvina
Laboratorio IDeAR. Facultad de Ingeniería, Universidad Nacional de Jujuy, S. S. de Jujuy, Argentina,

ABSTRACT

The drying and rehydration behavior of dried mangoes, the solute incorporation effect during rehydration and the applicability of Fick's second law to the adjustment of experimental data were evaluated. Slabs of mango were dried in a discontinuous operation at 45, 50, and 60 °C and two airflows: 15 m/s and 3.5 m/s. Samples were rehydrated in water, glucose solution or sucrose solution. The quality indices of WAC, DHC and RA during rehydration were determined. Drying of mango occurred during the falling rate period, in two stages independent of airflow used. There was a greater diffusion with increase in temperature and a minor effective diffusion coefficient when velocity airflow diminished. During rehydration of the dried product we observed that water incorporation was greater for glucose-rehydrated samples than for sucrose-rehydrated samples, and, in both cases, the obtained values were lower than the value for pure water. Sucrose- and glucose-rehydrated samples show a countervailing effect with respect to solid loss. Samples that were rehydrated in solute had lower WAC values than samples rehydrated in pure water, and diffusion was favored by solute incorporation. D_{eff} varied during the rehydration process along with the water content of the system. Sorption properties of dried mangoes were studied to evaluate the store conditions of the product. Sorption was conducted by the isopiestic method at 8°, 25° and 35°C. We observed isotherms of type J, which are characteristic of foods with high sugar contents. According to the sorption results, and considering frequently storage conditions for extreme times of the year, we can infer that when the weather is hot and humid, the temperature will not produce changes, but the humidity will have a negative effect.

Keywords

Diffusion, microstructure, air velocity, quality indices.

1. INTRODUCTION

Mathematic descriptions of dehydration are important to the design and optimization of drying processes. While the exact mechanism of moisture movement is still unknown, the most accepted theory is that it moves by diffusion through a concentration gradient. Some authors have assumed dehydration to be controlled by diffusion and analyzed their experimental data using Fick's diffusion laws. These studies demonstrated that a model based on first-order kinetics could properly describe the loss of water during dehydration [21, 12, 19, 20, 38, 75, 25, 73].

The assumption that the diffusion coefficient is constant during the drying process is not always valid. Some publication report the effective diffusion coefficient varies with sample moisture content [102, 32, 75, 29] and with operation temperature [83, 101, 71, 25, 91]. The usual way to introduce water diffusion temperature dependence is to consider the Arrhenius relationship with the reference diffusion coefficient (D_0) and activation energy (E_a).

To understand drying mechanisms, the external resistance to mass transfer must be negligible, which will assure with high rate of airflow. Some authors studied drying behavior assuming internal control conditions, using an airflow velocity between 1 and 5 m/s [102, 23, 97, 2, 8, 19, 72, 91]. However, other authors suggest that high airflow velocities (13–16 m/s) are necessary to minimize external resistance [38]. Under these conditions, it is possible to determine an instant drying rate.

During the process of dehydration, the water that has been removed is represented by different stages according to the degree of saturation of the food; the water removal cannot be considered to be a reversible process. The mechanism of moisture movement during dehydration is different from the mechanism of water movement during rehydration [23].

Several changes occur during the rehydration process, including mass transfer, water transfer from the liquid phase or solution through the food material and transfer of solids from the food to the solution. The simulation and commercial application of rehydration require knowledge of the mechanisms involved in these fluxes. For this reason, determination of the kinetics of the rehydration process is fundamental to the transfer of technology to food industries that use dried food products as feedstock.

The rehydration characteristics of dried materials are important for the determination of product quality and are used as quality indices of the physical and chemical changes that occur during the drying process where the sample composition, drying conditions and pretreatment conditions play important roles [66, 64, 92].

Besides the amount and rate of water absorption determine the sensorial properties and customer preparation/utilization times of various foods. It was demonstrated that the volume changes in biological materials due to rehydration are usually proportional to the amount of water that has been absorbed. During the process of rehydration, water absorption is rapid during the initial stages. This rate gradually decreases as the moisture content approaches equilibrium; near equilibrium, water has filled nearly all available pores, and the material has recovered a considerable percentage of its original moisture content [55]. However, during the process of rehydration, loss of solids also occurs, which can involve losses of vitamins, sugars, amino acids, and minerals. The loss of solids is a kinetic phenomenon with diffusion as its main mechanism; it occurs at a greater speed than water absorption [35].

Mathematical tools that allow us to represent rehydration processes are focused on the determination of water kinetics, which describes how certain process variables could influence water transference [51, 34]. Some authors describe rehydration for specific food materials, assuming water transport from the surface to the solid interior occurs mainly by diffusion, and they have determined effective diffusion coefficients using Fick´s second law [80, 79, 13, 55, 66, 13, 77, 78, 35, 37, 59].

Three indices are proposed to estimate the rehydration characteristics of dried products: absorption water capacity (WAC); dry-matter holding capacity (DHC); and rehydration ability (RA). WAC provides information regarding the capacity of the matrix to absorb water with respect to the water content after dehydration. The DHC index is a measure of a material's ability to retain soluble solids after rehydration and provides information regarding tissue damage and the tissue's permeability to solutes. Finally, the RA index expresses the hydration ability of a dried product and indicates the total damage caused by dehydration and impregnation during rehydration.

It is necessary to consider the changes of the macrostructure and microstructure of the tissues during processes, including the pretreatments applied before dehydration, the dehydration process itself and the rehydration process.

Every process that is used to conserve a food material is detrimental to its tissue integrity, particularly to the cellular membrane [89]; therefore, the characteristics of vegetal tissues are a key factor in mass transfer. The degree of rehydration depends on the grade of cellular and structure rupture due to the pretreatment and dehydration processes [13]; therefore, structural changes are associated with the specific properties of each rehydrated food.

The storage behavior of a dehydrated product is another index that allows its quality to be inferred under certain conditions, meaning that knowledge of its sorption properties is especially important. We can associate changes in the color, flavor, texture, stability and acceptability of a food product to the changes in a_w over small ranges [65, 93, 99].

Water sorption isotherms are highly specific for a given matrix and can change significantly, depending on the manipulation of the material under study. Mathematical models that represent sorption isotherms are useful in drying process design and often provide the parameters of the stability characteristics of storage materials; consequently, these models must be used to predict a product's shelf life. There are a number of models that allow the correlation of the equilibrium water content with aw, while also considering the influence of temperature. These models can be empirical, semi-empirical or theoretical. The BET (Brunauer, Emmett and Teller) model is one of the most commonly used models for foods with high sugar contents and is easily linearized and widely used to estimate monolayer water content and sorption heat [14]. The Henderson equation provides a good fit to foods with high sugar contents, but it involves empirical constants with no physical meaning [93]. The Iglesias and Chirife equation is used to adjust experimental data for high sugar content foodstuffs and provides good performance with these products (42, 41]. The GAB (Guggenheim, Anderson and de Boer) equation contains parameters with physical meanings, but it is complex and cannot be linearized. This equation has a thermodynamic basis and fits experimental data properly over a wide range of relative humidities [42, 62, 67, 96, 94, 99]. The standardization of the determination of sorption isotherms was presented many years ago by the Water Activity Group of the European Economic Community Project COST 90 [90, 49, 15]. At that time, the use of saturated solutions and the static method were adopted [62, 63, 81].

The Clausius-Clapeyron equation can be used to predict aw at any temperature if one knows the sorption heat for a given constant water content [94, 16, 43, 69, 85]. We can predict aw at any temperature through taking at least two isotherms with differences in temperature no greater than 10°C, using the Clausius-Clapeyron equation [41, 93, 7, 47, 39]. Thermodynamic relationships allow the estimation of process energy requirements and the prediction of optimal storage conditions to obtain maximum food product stability. Therefore, thermodynamic properties, such as enthalpy, Gibbs free energy and entropy are important for the design and optimization of a drying operation. Hubinger et al. [40] reported the sorption isotherms of mango slices dried in air at 50°C in a vacuum oven and rehydrated to different water contents using an aw electronic meter. They described mango isotherms at 25° and 50°C, and they found no temperature effect on thermal sorption behavior. The reversibility of dehydration and rehydration processes was assumed in this study. However, depending on the drying technique used, it is possible to obtain different product characteristics using the same original material, particularly with regard to its rehydration capacity [82].

The aims of this study were 1) to evaluate mango behavior during drying with airflow velocities of 3.5 and 15 m/s and three different temperatures, to determine their effects on mass transfer and 2) to evaluate the effect of solute in the rehydration process of dried fruit.

2. MATERIALS AND METHODS

We acquired mangoes from a local market in Jujuy Province, Argentina. The fruit was brought to the laboratory in wooden boxes and was refrigerated at 13ºC until it was used; the refrigeration time was no longer than four days. The sugar content was inferred from digital refractometer (ABBE Quartz, Belgium) measurements of soluble solids; the sugar content was expressed in ºBrix. The fruit was cut into 4 cm x 4 cm x 0.4 cm slabs (using the geometry of infinite slabs).

2.1 Moisture determination

Moisture content of samples was determined following the AOAC Nº 925.45 or 44.1.03 (1995) method in a vacuum oven (Shel lab, model 1410) at 60 ± 1 ºC and 25 in Hg of vacuum.

2.2 Drying of mango

The slabs of mango were subjected to thermal dehydration in a laboratory tray dryer with forced air convection at 45 ± 1º, 50 ± 1º and 60 ± 1ºC and air flow rates of 3.5 and 15 m/s, until equilibrium was achieved. An experimental dryer with a flow and air temperature control system was used for achieve the greater air rate. A DENVER APX analytical balance (200 g capacity and precision ± 0.0001g) was used to measure sample weights.

Weight loss (WL) and water content (w) were evaluated. Process kinetics was followed until the variation in weight loss was not significant.

2.2.1 Shrinkage

Shrinkage, which occurred during the dehydration process as a result of water elimination, was evaluated by determining the relative volume of the dried material (VR). The relative volume was the ratio of the mango slab volume after dehydration (V) to that observed before dehydration (V_0), as follows:

$$VR = V/V_0 \qquad (1)$$

The volume of each fruit sample was calculated by multiplying three basic sizes measured by a slide caliper. One hundred replicates were performed using samples with the same moisture content.

2.2.2 Mathematical model

Assuming isotropic diffusion, a constant effective diffusion coefficient (Deff), and constant temperature, Fick's second law for one-dimensional diffusion is (2) [21]:

$$\frac{\partial w_w}{\partial t} = D_{eff}\left[\frac{\partial^2 w_w}{\partial x^2}\right] \qquad (2)$$

Crank [21] proposed the solution of the Equation (2) for an infinite slab, under the following assumptions: (a) the initial moisture content in the solid is uniform, (b) the material keeps its original shape during dehydration, (c) the solid surface is continuously in equilibrium with drying air, (d) heat transfer occurs rapidly so it is negligible, (e) the effective diffusion coefficient is constant, and f) flow interactions are negligible. The solution proposed by Crank (2) is:

$$\frac{W-W_e}{W_0-W_e} = \frac{8}{\pi^2}\sum_1^{\infty}\frac{1}{(2n+1)^2}\exp(-\frac{(2n+1)^2}{4}\pi^2\frac{D_{eff}}{L^2}t \qquad (3)$$

Diffusion coefficients obtained using the first term of the mathematical series were not different from those obtained using 3, 5, and 7 terms of the series [102]. For simplicity, we restrict Equation (3) to the first term, resulting:

$$w = \frac{W-W_e}{W_0-W_e} = \frac{8}{\pi^2}\exp\left(\frac{D_{eff}}{4}\frac{\pi^2 t}{L^2}\right) \qquad (4)$$

Diffusion coefficient D_{eff} can be evaluated by plotting the logarithm of the first term of Equation (4) versus time. Its variation with sample moisture content can be obtained by mathematically correlating experimental data.

2.3 Rehydration

Rehydration was achieved by submerging the dehydrated samples in water or solution in a 30:1 ratio in glass containers with 250 ml capacities. The containers were maintained at a constant operating temperature and a constant agitation of 100 rpm in a Vicking shaker. The weights and water gains were evaluated from the variations in the water contents of the samples and losses of solids.

2.3.1 Effect of solute on rehydration process.

Dried mango samples were rehydrated in sucrose 60° Brix and glucose 35° Brix solutions at 25°C. We selected these concentrations of the solutes because they were commonly used in osmodehydration, to provide similar decreases en water activities.

Samples were weighed at different immersion times using an absorbent tissue to eliminate excess surface liquid. Weight and water gains were determined using the gravimetric method.

Due to the difficulty in measuring soluble solids using a refractometer and given the low moisture contents of the samples, especially at the beginning of the process, the total loss of solids was evaluated based on a mass balance of the system. The kinetics of the process was followed until the variation in weight gain was insignificant.

Each treatment was evaluated using a minimum of three replicates, and each replicate was tested in triplicate.

Dried mango that was rehydrated in pure water was used as a control system.

2.3.2 Structural analysis

Sample microstructures were observed by SEM. Small pieces that were taken from the inner parts of the mango slabs were fixed, fractured using liquid N_2, gold-coated and analyzed in a high vacuum using a scanning electron microscope (JEOL JSM-6480 LV; Japan).

2.3.3 Mathematical model.

We evaluated the fit of the experimental data to Fick´s second law solution for an infinite slab, assuming isotropic diffusion, a constant effective diffusion coefficient (D_{eff}) and constant temperature. We assumed that (a) the initial moisture content in the solid is uniform, (b) the material retains its original shape during the rehydration process, (c) the solid surface reaches moisture saturation immediately as it is submerged, (d) external resistances to mass and heat transfer are negligible, (e) the effective diffusion coefficient is constant, and (f) any change in the volume of the solid is negligible. Under these assumptions, the solution to (2) is the equation (3) (21, 102, 8, 38, 75, 12, 19, 20]. When analyzing our data, we assume that the series in (3) can be approximated by the first term, as in equation (4).

From a plot of log (W/Wo) vs. t, the effective diffusion coefficient (D_{eff}) can be evaluated, and the variation of the effective diffusion coefficient with the moisture contents of the samples can subsequently be obtained by mathematically correlating the experimental data.

2.3.4 Quality indices

The experimental relationship between the water absorbed during rehydration and the water lost during dehydration (WAC) was evaluated using the following equation:

$$WAC = \frac{m_{wr}-m_{wd}}{m_{wb}-m_{wd}} \qquad (5)$$

The DHC index (dry-matter holding capacity, g solids in rehydrated sample/g solids in dehydrated sample) was evaluated by:

$$DHC = \frac{m_{sr}}{m_{sd}} \qquad (6)$$

The rehydration ability was calculated by:

$$RA = WAC \times DHC \qquad (7)$$

Each treatment was evaluated by a minimum of three replicates, and each replicate was tested in triplicate.

2.4 Statistical analysis

Statgraphics Centurion XV and GraphPad Software were used for statistical analysis. Analysis of variance (ANOVA) and the LSD mean comparison test were used to determine differences between the treatments to find temperature effects during dehydration and solute effect during rehydration. The significance levels used were 0.05 and 0.01. Linear and non-linear regressions were used to develop an equation that related water diffusion coefficients and water absorption rates with water content. Each treatment was evaluated using at least three determinations with each in triplicate.

2.5 Determination of sorption properties

The isopiestic method was used to determine the sorption properties. Supersaturated solutions of prepared KNO_3, $BaCl_2$, KCl, NaBr, NaCl and LiCl were placed in containers that were suitable to saturate the atmosphere and to provide constant relative humidity to the selected microenvironment.

Fresh fruit sorption isotherms were determined. In total, 2.5 g of fruit was placed in a glass weighing bottle. Samples were previously treated with dilute sodium hypochlorite solution and were sprayed with a potassium sorbate (1,000 ppm) solution to limit microbial growth. Adsorption isotherms were evaluated using lyophilized samples and carried out in a Heto Lab Equipment FD4 model (Germany) to a constant weight. Fresh and lyophilized samples were placed in triplicate into the containers, 25 pulg Hg of vacuum was applied, and the temperature was maintained at 25±1ºC or 35±1ºC in the oven and 8±1ºC in the refrigerator. Samples were weighed at different times until stabilization to determine the equilibrium moisture content for each aw.

The temperature effect on sorption isotherms was evaluated by applying the Clausius-Clapeyron equation, which was deduced for liquid-vapor equilibrium, to the temperature-water pressure data. This method allows us to calculate the enthalpy changes associated with the sorption process for different moisture values (isosteric equilibrium). The Clausius-Clapeyron application is based on the following suppositions: (1) there are no changes in the pure water vaporization heat and sorption isosteric heat (ΔH) at different temperatures, and (2) the moisture content of the system remains constant.

$$\ln P = \Delta H / RT + c \qquad (8)$$

where c is the constant.

ΔH values were calculated for different moisture contents, and ΔG and ΔS values were determined using thermodynamics laws, while considering net isosteric heat reduction with increases in the moisture content.

$$\Delta G = \Delta H - T\,\Delta S \qquad (9)$$

The net sorption heat was calculated by

$$Q_s = \Delta H - \Delta H_v \qquad (10)$$

ΔH_v vaporization of pure water 54 enthalpy, kJ/mol

2.5.1 Isotherm mathematical models

Statistic software was used to correlate the data and obtain graphical representations of the experimental results. Sorption experimental data were adjusted by the GAB equation using an indirect method.

$$\frac{W_e}{W_m} = \frac{C\,K\,a_w}{(1-K\,a_w)\;(1-K\,a_w+C\,K\,a_w)} \qquad (11)$$

Sorption data were used to predict the behavior of the dried mango under storage conditions. A GAB parameter statistical analysis was conducted using the Statgraphics software. A basic descriptive analysis, a variance test and a T test were carried out with a significance level set at 95%.

The sorption surface area was calculated by

$$\sigma = A_{H_2O} \times N_{AV} \times \frac{W_M}{PM_{H_2O}} \qquad (12)$$

σ sorption surface area, m^2/g; NAV Avogadro's number = 6 x 10^{23}; W_M monolayer water content g/100 g dry basis (db); A_{H2O} surface of a water molecule = 1.06 10^{-19} m^2

3. RESULTS AND DISCUSSION.

Initial air conditions at each of the three temperatures used are shown in Table 1. The absolute humidity of air used for drying was similar in all cases.

Equilibrium values of moisture content for samples dried with 15 m/s air flow are 0.053±0.001, 0.034±0.001, and 0.025±0.001 g/g d.b. for 45, 50, and 60 °C, respectively. The kinetics of the elimination of moisture was similar at the three temperatures evaluated (Figure 1). Sample stabilization began at 3600 (60 min), 5100 (85 min) and 5400 (90 min) seconds for 60, 50, and 45 ºC, respectively. After 30 minutes of there was no statistical difference between response curves obtained at 45 ° and 50 °C. Water content of the samples decreased with increasing temperature until 95 minutes of drying time. After that time, the temperature effect was negligible, which indicates that operations at high temperatures require less time to achieve the same moisture content in the fruit. This is similar to the reports of Prachayawarakorn et al. [75] in banana, Vega-Gálvez et al. [95] in red pepper, Biju Cletus and Carson [12] in chestnuts, Kaya et al. [46] and Orikasa et al. [71] in kiwi, Seremet et al. [82] in pumpkin slices.

Table 1: Drying air conditions

Ts_{ou} K	HRs_{ou} %	T K	HR %	Ha kg/kg d.a.	h kJ/kg d.a.	w_f g/g d.b.
295	70.8	333.15 (60 °C)	8.5	0.011	106.6	0.077
294	77.6	323.15 (50 °C)	14	0.0115	96.1	0.17
294	77.7	318.15 (45 °C)	21	0.012	92.0	0.13

Sou: sourround; *HR*: relative humidity; *Ha*: absolute humidiy; *h*: enthalpy; w_f: final water content

Fick´s second law provided a satisfactory adjustment of the experimental data as found in other food matrices [88, 8, 23, 71, 9, 104, 38, 64, 73].

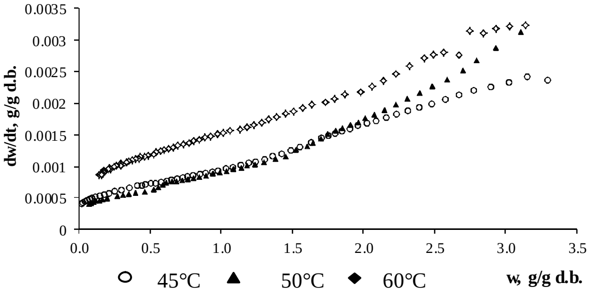

Figure 1: Drying curves of mango (15 m/s). Temperature effect.

To verify assumption (e) in Equation 4, the variation of effective diffusion coefficient with time was evaluated. This variation depended upon moisture content as suggested by the nonlinear shape of the experimental data. This behavior is similar to that observed by Krokida and Marinos-Kouris [51], Giraldo et al. [37] and Doimaz [25]. We found that the variation of the diffusion coefficient with water concentration obeyed a linear relationship, at each of the three used temperatures.

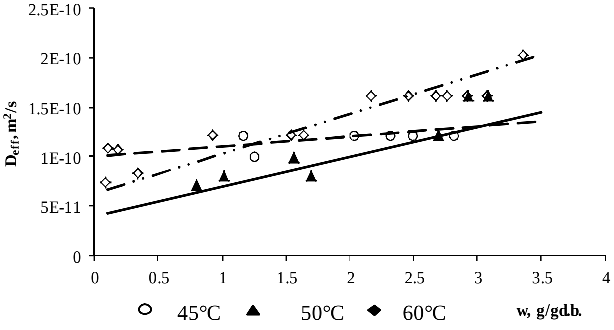

Figure 2: Effective diffusion coefficient. Temperature and water content effects.

Effective diffusion coefficients and the effects of temperature and water content evolution can be observed in Figure 2. These values are similar to values reported for others fruits: apricot drying at 60 °C with air flow 0.5 m/s, $D_{eff} = 5.59\ x10^{-9}\ m^2/s$; for banana at 50 ºC, air flow 3.1 m/s and 10 – 35 % of air relative humidity, $D_{eff} = 4.6\ x10^{-10}\ m^2/s$, kiwi at 60 ºC and air flow 3 m/s , $D_{eff} = 9.46x10^{-10}\ m^2/s$; for apples $D_{eff} = 2.93x10^{-10} - 6.08x10^{-10}\ m^2/s$ for drying temperatures of 55, 65 and 75 ◦C and a constant air velocity of 2.0 m/s [23, 83, 8, 25] . The effective diffusion coefficient reported for orange skin varies between $0.81\ x10^{-10} - 5.11\ x10^{-9}\ m^2/s$ using temperatures between 30–90 °C. González-Fésler [38] reported $D_{eff} = 3.3x10^{-11}\ m^2/s$ for apples drying with air at 60 °C and 9-10 % relative humidity. Corzo et al. [19] studied water diffusion in mango at two stages of ripening drying with 60 °C and 1.8 m/s air and report D_{eff} of $1.74x10^{-10}$ and $2.30x10^{-10}$ for green and half-ripe stages. The effective diffusion coefficient increased with temperature as reported by other authors [19, 46, 101, 95].

No drying constant period was found as reported for other matrixes [88, 8, 32, 91]. Drying of mango occurred during the falling rate period as other authors report for other matrixes [8, 70, 20, 73]. Results showed that water movement was controlled by diffusion.

Figure 3 shows the water elimination rate (dw/dt) with moisture content. Slope changes affirmed that drying occurred in two stages during the falling rate period demonstrating a hygroscopic behavior of mango where water was transferred from the solid centre to the surface as vapor. The first stage had a higher water elimination rate and was complete after 25 and 30 minutes of operation.

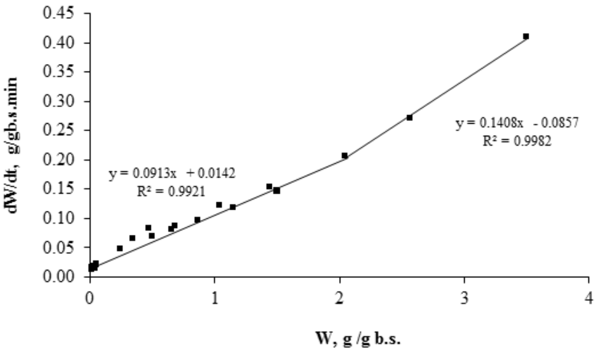

Figure 3: Drying curves of mango (3.5 m/s, 60ºC).

Water diffusion was similar at 50 ° and 60 °C. Drying with air at 45 °C produced minor water diffusion due to minor heat transference that influenced mass transfer velocity. The variation of the effective diffusion coefficient with temperature fits the Arrhenius equation as found with other matrices [9, 84]. The activation energy obtained was 17.58 kJ/mol, which is in the range to that previously reported for mango and other fruits: Ea (kiwi) = 27 kJ/mol – 29.6 kJ/mol, E_a (orange skin) = 37.1 kJ/mol, E_a (apple) = 24.51 kJ/mol, Ea (sweet cherry)= 43.05 kJ/mol; Ea (fig) = 40.95 kJ/mol), E_a (green mango) = 22.3 kJ/mol, E_a (ripe mango) = 9.3 kJ/mol, and E_a (mango) = 8.30 kJ/mol [102; 83, 101, 19,20, 71, 103, 25]. Similar to results reported in this study, early reports of Labuza [53] and Roberts and Tong [76] show that a diffusion controlled process has an E_a value less than 34 kJ/mol. Water effective diffusion coefficient increases with T in the studied range. Hence drying process is accelerated with increase in T.

Effect of air rate

Industrial scale drying processes use air rate near 3.5 m/s. Water elimination control in this situation is expected to be joint between internal and external control. This means that two transferences could take importance: 1) water migration rate from the inside and through the pores, as liquid or as vapor, produced by concentration differences, pressure gradient or capillarity and 2) vapor water transfer velocity form the surface layer through the air.

We studied drying of mango with airflow of 3.5 m/s to evaluate deviation from the ideal situation. We do not observe a constant rate period, similar to Desmorieux et al. [24] reports related to studies of semi-industrial drying of mango al 60 ºC and similar to results obtained with high air velocity (15 m/s).

In order to analyze the presence of more than one falling rate period we applied linear and no linear regression to experimental data to determine slope changes. Figure 3 shows that drying of mango with 3.5m/s airflow presents two stages for the falling rate period in coincidence with founded for drying at high air velocity, in case of internal control. At the beginning of the process velocity is higher until samples reach a water content of 2 g/g b.s. in almost 30 minutes, then velocity diminish slowest.

Figure 4 compares effective diffusion coefficients for high and lower velocity. There is a greater diffusion with increase in temperature and a minor effective diffusion coefficient when velocity airflow diminishes. However these values are similar to other food, as reported by Kaya et al. [46] Orisaka et al. [71] and to some previous result obtained for mango [102].

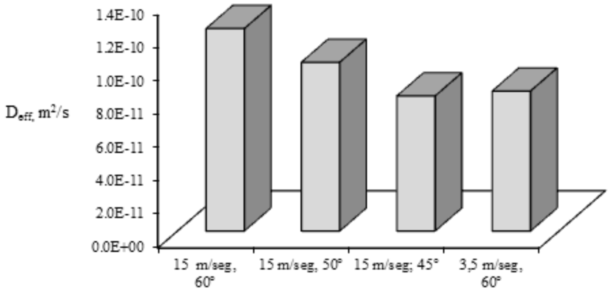

Figure 4: Effect of temperature and airflow on effective diffusion coefficient.

Effective diffusion coefficient varies with moisture concentration as:

$$D_{eff} = c1\ \ W + c2$$

c1 and c2, constants

The effect of moisture content is greater when velocity is lower. Working with airflow of 15 m/s temperature effect is greater. The values obtained for drying with air at 60ºC and 3.5 m/s were c1: $7.0\ 10^{-9} \pm 1.0\ 10^{-11}$ and c2: $1.310^{-24} \pm 1.510^{-25}$; for drying at 60ºC and 15 m/s c1: $410^{-11} \pm 1\ 10^{-14}$; c2: $610^{-11} \pm 1\ 10^{-14}$ and for 50ºC – 15 m/s the values were c1: $310^{-11} \pm 1\ 10^{-14}$; c2: $410^{-11} \pm\ 1\ 10^{-14}$

After dehydration moisture content of the samples results 0.047 ± 0.007 and 0.025±0.001, for 3.5 m/s and 15 m/s, respectively. Molecular diffusion of water is bigger when air velocity increase, in coincidence with that observed for Kaya [46] in kiwi. Changes en water elimination velocity during first stage of falling rate drying period is superior to the second stage.

We verify the assumption that internal resistance to mass transfer is significant and that the external resistance is negligible, analyzing the Biot number and considering:

$$Bi^{mass} = k_m \,.\, L/\ D_{eff}$$

and

$$h/c_p \,.\, Pr^{2/3} = \rho \,.\, k_m\, Sc^{2/3}$$

where, k_m: coefficent of mass transfer, m/s; L: thickness slab; Pr: Prandtl number; Sc: Schmidt number.

Knowing water properties for the used range of temperature we estimate:

$$Pr^{2/3}/\ \rho.\ c_{p.}\ Sc^{2/3}\ \approx 0{,}001\ \ »\ \ k_m \approx h\ .10^{-3} \approx 0{,}015 - 0{,}03$$

The obtained values for Bi^{mass} were: 8.32 105; 6.66 105, 5.56 105 for drying with air velocity of 15 m/s and 45°, 50° y 60° C, respectively. Drying with airflow of 3.5 m/s and 60ºC showed a Bi^{mass} number of 8.04 105. These values demonstrate internal mass transfer as predominant factor during drying and allow us to express that there is no significant differences in the mechanism of mass transfer due air velocity. Fick equation is valid to represent experimental data as in case of observed by Biju Cletus and Carson [12] in drying process of chestnuts. We used the criteria of Sun and Meunier [86] to evaluate prevalence of mass or heat transfer. We used Lewis and $Biot^{heat}$ numbers and the number obtained multiplying both. Lewis number for drying with air 3.5 m/s and 60ºC results: 1.01 and for 15 m/s result: 1.05, 83.9 and 69.9 for 45º, 50º and 60º, respectively. These results allow us to explain the differences found in diffusional behavior during drying at the lower temperature and the higher velocity, situation in which heat transfer became relevant. We evaluated $Le \times Bi^{heat}$ values, resulting: $2.17\mathrm{x}10^2$, for 60ºC and 3.5 m/s; $2.24\mathrm{x}10^2$, $1.80\mathrm{x}10^2$, $1.50\mathrm{x}10^2$, for 15 m/s and 45º, 50º and 60ºC, respectively. These values show that mass diffusion is sufficient to describe drying process of mango.

Rehydration. Effect of solute

After the mangoes were dehydrated but before they were rehydrated, the samples reached a moisture content of 0.047±0.007 g/g d.b.

According to the obtained results, the rehydration kinetics show typical behavior with a high initial absorption rate followed by a slow absorption rate (Figure 5a and 5b) in accordance with other reports [34, 68, 6]. This asymptotic behavior is related to a mass transfer driving force reduction with rehydration time and close to system equilibrium. Quick initial absorption occurs due to the filling of capillaries over the sample surface. As water is absorbed, the hydration rate decreases, due to the filling of capillaries and intercellular spaces. The dehydration process produces cellular shrinkage and alterations in the cell walls. When the material is rehydrated, the cells absorb water in relation to the damage sustained.

The equilibrium moisture content (saturation) of the samples was different from the initial mango moisture content, reaching 75.7% of the original water content. This finding confirms the irreversibility of the process and the structural damage that occurs during dehydration as was demonstrated for other matrixes [10, 95, 51]. We obtained a water gain of 2.8±0.1 g/g (d.b.), weight gain of 2.1±0.2 g/g (d.b.) and solid loss of 0.7±0.1 g/g (d.b.) at equilibrium. The aw value of the rehydrated samples, which was evaluated at 25°C, was 0.994±0.001.

We obtained greater weight gains for the samples rehydrated in glucose solution than for the samples rehydrated in sucrose solution in accordance with behaviors reported by Atarés et al. [6], for other fruits. This finding could be due to the higher concentration of the sucrose solution, indicating that the driving force of the process (water concentration gradient) results was weaker. Systems with solute incorporation present less weight gain than control samples; this situation has a linear relationship with the driving force of water flux in each case.

Water incorporation was greater for glucose-rehydrated samples than for sucrose-treated samples, and, in both cases, the obtained value was lower than the value for pure water. These effects are shown in Figure 5a. Water mass transfer was higher during the first hour of operation; the transfer rate significantly decreased with time until equilibrium was reached, coincident with other reports for vegetal products where mass transfer occurs between 30 and 60 minutes of treatment [55, 60]. Water diffusion from the liquid to the solid surface and subsequently to the solid interior was affected mainly by the solution concentration, which affects the aw of the rehydration medium. Other variables, such as geometry, sample size, porosity, tortuosity, temperature and agitation, can influence water diffusion, but they were not considered in this study because they were maintained at constant levels for the duration of the study.

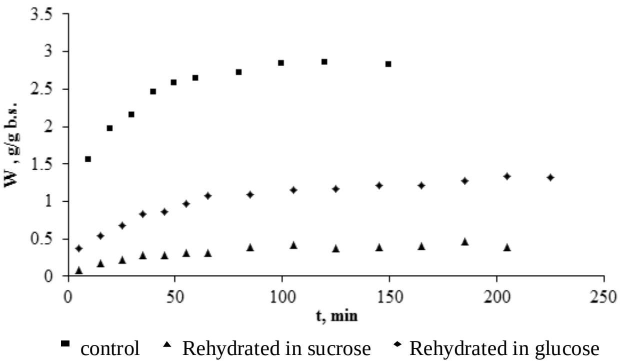

Figure 5 a: Evolution of water content during rehydration of mango (25ºC). Effect of solute incorporation

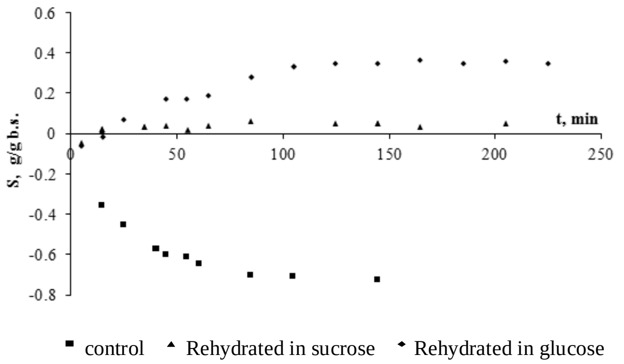

Figure 5 b: Solids gain/loose during rehydration at 25ºC. Effect of solute incorporation.

Sucrose- and glucose-rehydrated samples incorporated less water than did control samples, due to increases in the resistance to mass transfer. This resistance was due to the film that formed adjacent to the fruit, which was caused by the presence of solute in the rehydration solutions, making the driving force (given by the difference in the chemical potential between the solution and the food) less prevalent. The equilibrium moisture contents were 2.9, 1.3 and 0.4 g/g (d.b.) for the samples that were rehydrated in pure water, glucose and sucrose, respectively. These values correspond to the saturation level of the matrix in equilibrium with the rehydration liquid.

The initial water content was not reached in any of the samples, and the amount of incorporated water was approximately 80% of the initial water content. This finding indicates the irreversible damage produced by dehydration, which results in a loss of rehydration ability according to Krokida and Marinos-Kouris [51] and Figiel [30]. In this analysis, it is important to highlight that the aw of the sucrose solution was less than the aw of the glucose solution (0.895 and 0.945, respectively), which is a finding related to the chemical potential and, therefore, to the driving force of the process.

Sucrose- and glucose-rehydrated samples show a countervailing effect over solid loss compared to the control sample that was rehydrated in pure water. We obtained a gain of solids after five minutes of operation for both solutes. The gain was greater for glucose-rehydrated samples in which diffusion is favored by a smaller molecular size and lower solid concentration with a consequent decrease in the candying effect (Figure 5b). Solid loss prevailed in the initial minutes, influenced by a loss of physical material as a result of the textural damage suffered by the matrix during the dehydration process.

The values of gained and lost solids were determined after considering the final solid content of the dehydrated product as the initial solid content of the rehydrated product.

Glucose-rehydrated samples had a higher gain of solids and higher water incorporation than did sucrose-rehydrated samples, which is consistent with their greater gain in weight. By analyzing accelerations, or changes in the water incorporation velocity, we can infer that rehydration in water at 25°C occurs in a unique decreasing rate period. Control samples reached a water content of 2.5 ± 0.1 g/g (d.b.) and lost 0.61 ± 0.01 g/g (d.b.) of solids after 40 minutes of rehydration. These values represent 87.9% and 85.9% of the total incorporated water and total lost solids, respectively, when the process is close to equilibrium.

We found a decreasing rehydration rate with an increase in the water content in all cases, which, after 10–15 minutes, follows a linear relationship:

$$dW/dt = a + b\,W$$

The obtained values are 0.25 ± 0.03, 0.0161 ± 0.0005, and 0.059 ± 0.005 for *a* and 0.084 ± 0.009, -0.032 ± 0.002, and -0.041 ± 0.003 for *b* in the control, sucrose-rehydrated and glucose-rehydrated samples, respectively. This analysis is similar to the report of Krokida and Marinos-Kouris [51] in which they proposed a first-order equation to describe mass transfer during rehydration.

The water incorporation rate in the glucose system was higher than the rate observed in the sucrose system but was lower than the rate obtained in the control system.

The relationship between water incorporated during rehydration and water loss during dehydration (WAC) is shown in Figure 6. The equilibrium value is 0.726±0.003 for the control system, which indicates the elevated capacity of dehydrated samples to incorporate a portion of the water lost during dehydration, considering the collapse of tissues and cellular alterations caused by the thermal effect. The water absorption capacity was high in glucose-rehydrated samples, but samples that were rehydrated in solutes present lower WAC values than samples that were rehydrated in pure water over the entire evaluated range. This finding was due to the solute's effect over the availability of water. Figure 7 shows the DHC index evolution. The solid retention value after water rehydration (equilibrium) was 0.34±0.09. This value is due to the loss of solids and textural damage during food processing, resulting in a loss of tissue integrity, which produces small portions of lost material during rehydration.

We verified that the loss of solids in pure water rehydration is countered by solute incorporation into the rehydration liquid. This effect is evident after 10–15 minutes of rehydration. Solid incorporation during sucrose rehydration balances the losses that occur during dehydration and rehydration. Glucose-treated samples present a high solid retention index after 25 minutes of rehydration and for the rest of the evaluated period.

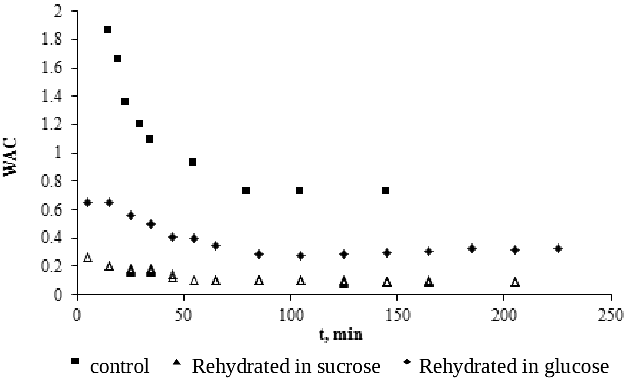

Figure 6: Water absorption capacity of rehydrated mango at 25°C. Effect of solute incorporation

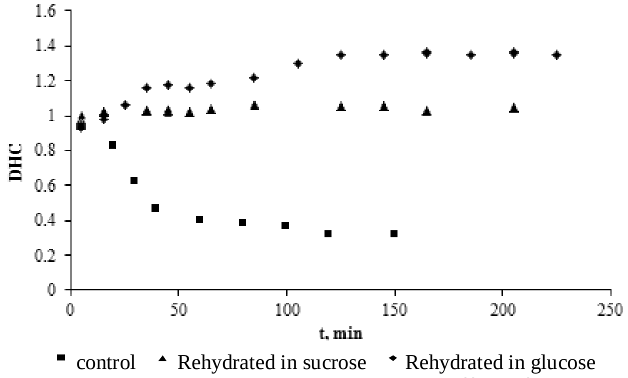

Figure 7: Dry-matter holding capacity. Effect of solute incorporation.

Atarés et al. [6] found similar WAC values in apple samples that were rehydrated in glucose and sucrose solutions, and they found low DHC values for the glucose solution.

The rehydration ability (RA) was calculated using the WAC and DHC values. The final value obtained for the control system was 0.334, which indicated irreversible damage produced by dehydration. The RA of glucose samples was identical to that of the control system (0.38) for the first hour. After that point, the glucose system is stabilized, but the RA of the water-treated samples continues to decrease. The RA of glucose-treated systems was lower than the values for other systems, but it implies a 7.6% increase in the first 15 minutes followed by a subsequent decrease until the value approaches 0.1 from the first hour. This value remains constant until the end of the rehydration process. The rehydration of mango slabs can be considered complete between 80 and 100 minutes of operation according the values obtained for the following evaluated parameters: weight gain, water gain, solid retention, water absorption and rehydration ability for both solutes (sucrose and glucose). Rehydration is coincident with the decrease in driving force related to the differences in chemical potential.

Rehydration mathematical models consider that water transport, which runs from the surface of the solid to its interior, occurs mainly by diffusion, verifying the applicability of Fick's second law in accordance with other studies [79, 80, 13, 34, 35, 61, 18, 22, 64].

The diffusion model (based on Fick´s second law) adjusts first-hour experimental data for pure water rehydration with a correlation coefficient of $R^2 = 0.9402$ according to other reports [66, 13]. The effective diffusion coefficient (D_{eff}) was $1.46 \pm 0.02 \times 10^{-10}$ m^2/s. We observed high levels of water diffusion through the solid during the first hour, which is evident in the effective diffusion coefficient values in all cases. Diffusion is favored by solute incorporation as seen in the D_{eff} values: we obtained higher D_{eff} values in solute systems than in pure water systems. These values are similar to other reports for water diffusion during various the rehydration processes of various vegetables, including date palms (between15×10^{-9} and 6.66×10^{-10} m^2/s for three varieties studied at 15°-45°C), yams (2.4×10^{-10}), and potatoes (2.6×10^{-10}) [48, 50, 45, 22].

Sucrose-rehydrated samples had higher effective diffusion coefficients than did the glucose-rehydrated and control samples. Solute incorporation produces an increase in water diffusion. D_{eff} values were 2.47 ± 0.09 10^{-10}, 1.81 ± 0.04 10^{-10} and 1.24 ± 0.04 10^{-10} m^2/s for the first hour of treatment in sucrose, glucose and control systems, respectively. For the rest of the evaluation period in the same systems, the values were 3.11 ± 0.01 10^{-11}, 1.80 ± 0.03 10^{-11} and 1.08 ± 0.03 10^{-11} m^2/s. According to these results, we affirm that the effective diffusion coefficient of water varies over time during rehydration, and this variation can be associated with changes in the system water content:

$$D_{eff} = c_1 + c_2 W$$

where c1 and c2 are constants.

We obtain values of $9.5 \pm 0.7 \times 10^{-10}$ and $-2.5 \pm 0.7 \times 10^{-9}$; $4.6 \pm 0.1 \times 10^{-10}$ and $-3.3 \pm 0.6 \times 10^{-10}$; and $7.5 \pm 0.7 \times 10^{-10}$ and $2.5 \pm 0.7 \times 10^{-10}$ for c_1 and c_2 in sucrose-, glucose- and control-rehydrated samples, respectively. We observed that the water content effect was more pronounced when sucrose was added to the rehydrating solution. When glucose was incorporated, we observed a similar effect to that of the control system. We found a moisture content value that made the effects of diffusion equal; in sucrose-glucose systems and sucrose-control systems, the moisture content values were 0.223 g/g (d.b.) and 0.089 g/g (d.b.), respectively. Variations in the diffusion coefficient with the moisture content were more pronounced when sucrose was used in the rehydration solution. This effect could be due to the molecular size and steric effects of sucrose, which may lead to less diffusion and a low aw of the solution as a result of the high sucrose concentration. This situation increases a candying effect and, therefore, decreases diffusion. Structural damage produced by dehydration caused a loss of integrity, which is evident during and after rehydration as suggested by Lewicki (1998). The cellular structure was affected by dehydration in several aspects: crystallinity modification of the cell wall, microfibrils and middle lamella, functionality loss of plasma membrane, due stress and loss of turgor; protoplast inability to expand and regain its original volume; tissue shrinkage; membrane lysis and vesiculation during rehydration; starch gelatinization; fusion; and redistribution of lipids.

We observed that dehydration produced fruit shrinkage. The variation in the volume of a sample is a measure of its level of structural tissue damage and cellular collapse. We found an overall level of shrinkage of 56 ±2%.

After analyzing microscopy results, we affirm that the control samples present cells of different shapes (circular, polygonal and elongated) to a lesser extent than the other systems (Figure 8).

Convection dried samples show collapse, cellular damage, cavity formation and shrinkage, as reported by other studies [28, 1, 57, 44] (Figures 9 and 10). Cellular rupture is due to damage to the membrane and cell wall and microstress caused by water elimination. This rupture involves cavity formation of different sizes and shapes, which increases sample porosity. Samples that are dried with air current present high levels of shrinkage (L1/L2 is half of the untreated sample). Changes in pore shape were observed by Thuwapanichayanan et al. [87]. These authors report that drying affects pore shape, due to thermal stress. We observed that the changes in the structural dimensions caused by drying are not isotropic.

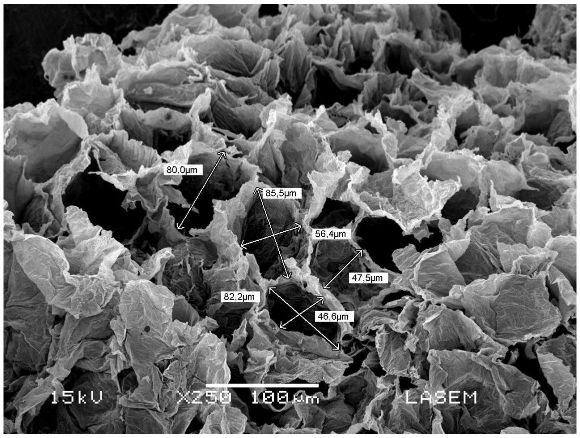

Figure 8: Microstructure of fresh mango (control) 250x.

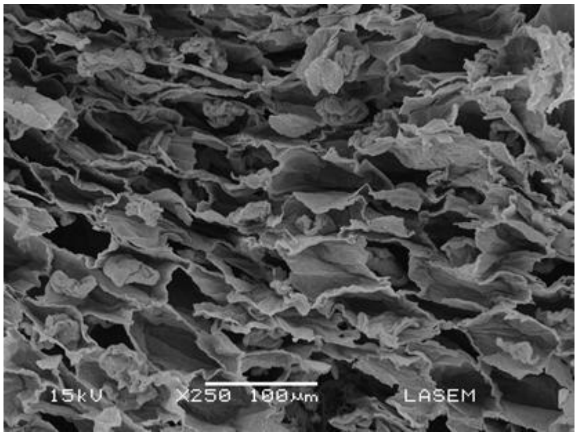

Figure 9: Microstructure of hot air dried mango (60°C) 250x.

Knowledge of the changes in mechanical properties is important because these changes are related to the sensorial and textural characteristics of the fruit and, therefore, to product quality and customer acceptance. Structural changes also affect water sorption properties and are related to the final texture of the product.

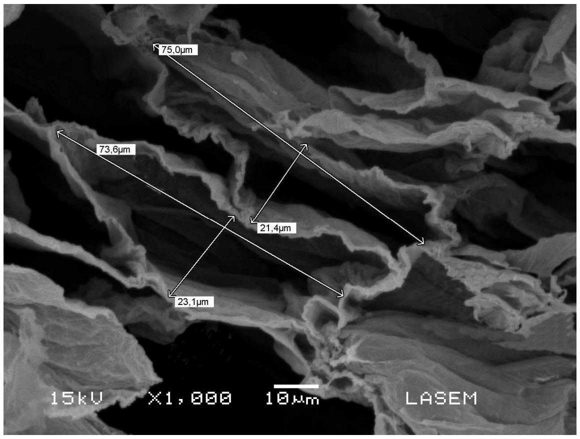

Figure 10: Microstructure of hot air dried mango (60°C) 1000x

Giraldo et al. [36] studied the microstructure of dried mangoes and reported difficulties distinguishing cells, which appeared to be collapsed. The boundaries between cell walls and membranes were also difficult to distinguish. The observed structural changes are the cause of the rehydration abilities and water absorption capacities of the samples.

We used the results of the sorption phenomenon evaluation to infer dried mango behavior under storage conditions at three different temperatures. Probable environmental temperatures throughout the entire year were selected as storage temperatures. Figures 11a and 11b show the sorption isotherms of mangoes at the three studied temperatures. We observed isotherms of type J, which are characteristic of foods with high sugar contents. The hysteresis effect was not significant at 25° or 35°C. The same behavior was observed by López-Malo et al. [58] in apple and papaya sorption isotherms. They found no hysteresis when fruits were previously blanched, but they observed hysteresis when the fruits were previously dehydroimpregnated.

An increase in temperature from 8ºC to 25ºC resulted in a lower equilibrium moisture content for a given aw, indicating that the fruit became less hygroscopic, as reported for other matrices, such as gingerbread (a sweet biscuit with a high sugar content) [16], potato [43], and chestnut [68]. This phenomenon may be due to the reduction in active sites for water binding as a result of the physical and chemical changes caused by temperature effects. In other words, the activation of water molecules changes to higher energy levels at higher temperatures, and bonds become less stable and leave the binding sites of the material. As a consequence, the equilibrium moisture content decreases. A further increase in temperature to 35°C had little effect on the sorption characteristics. The weak influence of temperature in the range of 25°C-35°C coincides with that reported by Hubinger et al. [40] regarding the behavior of sorption on pineapple, guava and mango.

Adsorption isotherms intersect, due to the higher solubility of sugars and aw values above 0.9. This effect was observed for African mangoes [27] and other foods with high sugar contents, such as bananas [26, 16]. The dissolution of sugars increases the surface tension, resulting in a lower water activity for a given moisture content. The swelling of polymeric materials during water adsorption can cause hysteresis, which varies with temperature. According to our results, we obtained higher hysteresis values at 25°C than at 8°C, in keeping with the reports of Yan et al. [104] for bananas.

The GAB equation parameters for desorption and adsorption curves at the three studied temperatures and obtained by nonlinear regression of data are presented in Table 2.

Table 2: parameters of GAB equation for desorption and resorption at 8 °, 25 ° and 35ºC

		W_M	C	K	R^2
8 ºC	Resorption	8.513	1.731	0.981	0.9706
	Desorption	6.255	1.791	0.989	0.9663
25 ºC	Resorption	6.699	0.435	1.033	0.9968
	Desorption	5.458	0.893	1.040	0.9836
35 ºC	Resorption	6.651	4.016	1.004	0.9602
	Desorption	6.773	2.742	1.026	0.9434

The GAB equation adequately fits experimental data over the entire range of studied a_w, in agreement with other reports [74, 16, 95, 43, 39, 17, 63, 100]. Monolayer water contents were lower than 10% (d.b.) and decreased with increasing temperature as observed by Moreira et al. [69]. K values give a measure of the interaction between the multilayer molecules with the adsorbant and are between the values of monolayer molecule vaporization energy and liquid water. The multilayer molecules have the properties of pure water when K is equal to 1. K values greater than 1 have no physical basis.

The average value represents all data with regard to the confidence intervals obtained for the parameters for both adsorption and desorption. The monolayer water content at 25°C and 35°C are not significantly different in the case of adsorption. These values differ statistically from the monolayer water content obtained at 8°C. K and C values are statistically different for the three evaluated temperatures.

Desorption data statistical analyses show that monolayer values have no differences between temperatures. K values at 25°C and 35°C are not significantly different. These two values statistically differ from the K value obtained for 8°C.

An analysis of variance was also conducted to assess the statistical similarity of the average monolayer value obtained for the three evaluated temperatures, finding no significant difference between the average experimental value obtained for the monolayer moisture during desorption and resorption at the three temperatures studied except in the case of monolayer moisture during resorption at 8ºC.

The surface area values obtained from the values of monolayer moisture adsorption and desorption at each temperature were 300.79 and 221.01, 236.70 and 192.85, and 235.00 and 239.31 for 8°, 25° and 35°C, respectively.

The high value of the area obtained is due to the microporous structure of the matrix. The values are similar to those reported by Cervenka et al. [16] and higher than those reported by Kumar et al. [52]. The adsorption surface area decreases with increasing temperature in the evaluated range; however, the values obtained for 25°C and 35°C are notably similar. These results indicate that the surface area available for hydrophilic bonding during adsorption decreases when the temperature increases from 8°C to 25°C/35°C. The desorption area decreases when the temperature increases from 8°C to 25°C. The highest value of desorption surface area was obtained at 35°C. Similarly, Arslan and Togrul [5] found no correlation between area and temperature for desorption. The increase in the area means that there are more charged and polar groups and carboxyl functions exposed, thereby increasing the amount of water sorption.

The values of surface area are higher for adsorption than for desorption, in keeping with the values of monolayer moisture.

The surface area plays an important role in determining the properties of bound water. The values obtained by Arslan and Togrul [5] were between 286 and 306 for adsorption and between 373 and 402 for desorption at the same temperatures evaluated in this study.

We verified a linear relationship between ΔH and 1/T using Clausius Clapeyron´s equation. ΔH and ΔG representations (Figures 12 and 13) show similar shapes as in other reports, presenting a maximum, near-monolayer water content at 25°C. Negative values for the variation in Gibbs's free energy were obtained, indicating the spontaneity of the process. ΔG values were higher with the increase in equilibrium moisture content (–1.849 KJ/mol K for 5 g/100 g (d.b.) and –0.376 KJ/mol K for 45 g/100 g (d.b.)).

The values for the change in entropy (Figure 14) denote a greater spatial rearrangement of the solute-water interface. There is strong dependence on entropy with moisture content, in keeping with the behavior reported by García-Alvarado et al. [33], Al-Mahasneh et al. [3], Al-Muhtaseb et al. [4], Kaya and Kahayaoglu [47] and Goula et al. [39].

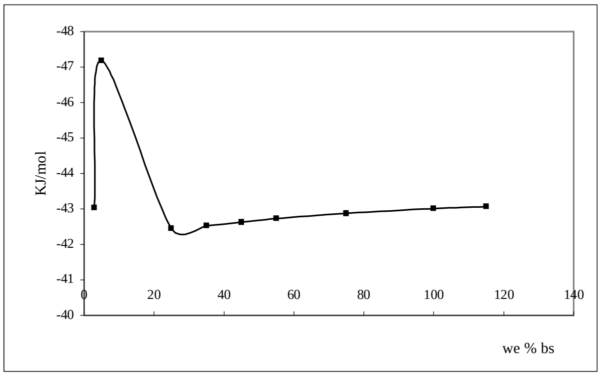

Figure 12: Isosteric heat change with equilibrium moisture content (25°C)

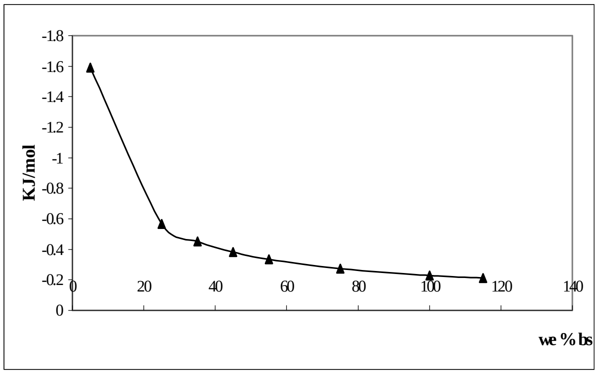

Figure 13: Gibbs free energy change with equilibrium moisture content (25ºC)

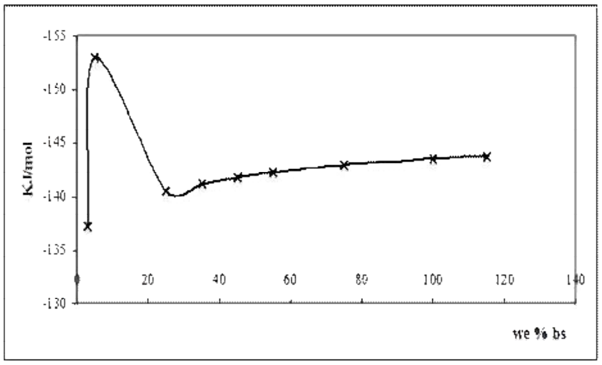

Figure 14: Entropic change with equilibrium moisture content (25ºC)

We found a liner relationship between ΔH and ΔS with the following correlation:

$$\Delta H = 0.275 \text{ x } \Delta S - 4.4314 \qquad R^2 = 0.9801$$

This finding means that we can apply the compensations theory in the evaluated moisture range. The kinetics compensation effect was also observed in such areas as physics, chemistry, biology and thermal analysis. Labuza et al. [54] evaluated the compensation applicability and described the problems that can be found by applying the concept of enthalpy-entropy linear compensation in reactions related to the thermal inactivation of microorganisms, protein denaturation and ascorbic acid degradation in foods. Fontan et al. [31] suggested an enthalpy-entropy linear relationship using a sorption equation of two parameters, including the effect of temperature on vapor water sorption.

The linearity of the relationship reveals a unique mechanism of controlled adsorption enthalpy as suggested by Beristain et al. [11] to study the relationship or enthalpy-entropy compensation in foods with high sugar contents (figs, apricots, prunes, raisins and dry goods). This relationship also suggests that foods with high sugar contents have more stable microstructures and that the sorption mechanisms of water will not change in the food within the evaluated temperature range.

Linear regression to enthalpy-entropy has an intercept value close to zero, which indicates sugar solubilization at high water contents and the conversion of an exothermic sorption mechanism into an endothermic mechanism (with heat change caused by the dissolution of sugars).

The sorption heat decreases exponentially with increasing moisture content and tends toward the value of pure water, indicating that the water is freer and more available as the water content increases, thereby coinciding with results found in other studies [52, 85, 39, 69]. At first, the decrease quickly reaches a moisture content of 25 g/g (d.b.) and subsequently decreases slowly, reflecting the difference in water binding forces. This phenomenon can be attributed to the fact that sorption initially occurs in the most active sites, thereby achieving the greatest interaction energy. At the beginning of sorption, water mostly occupies the polar active sites on the surface (with high interaction energy) and later occupies less available sites with lower binding energies, which are progressively filled. As the moisture content increases, the bond strength of water molecules and the heat of sorption decrease.

The sorption heat obtained for untreated mango was 10.492 kJ/mol for moisture values that were close to the monolayer water content. Yan et al. [105] reported a sorption heat variation range between 0.85 (W= 20% d.b.) and 7.67 kJ/mol (W= 10% d.b.) for bananas. Sinija and Mishra [85] reported values of 48.54 to 44.71 kJ/mol for moisture between 1% and 9% (d.b.) for green tea powder. Goula et al. [39] found a value of 42.9 kJ/mol for 12% (d.b.) and 7.4 kJ/mol for 36% (d.b.) for tomato pulp. These reports demonstrate a wide variability in published values.

If we investigate the storage of dried mangoes without packaging under environmental conditions and for extreme times of the year, we can infer its behavior. According to the sorption results, we affirm that during the winter (dry and cold weather), the product will not undergo significant changes in aw but will increase its equilibrium moisture content slightly. In the summer (hot and humid weather), the temperature will not produce changes, but the humidity will have an effect, leading to high aw values, which increase the risk of deterioration. For this reason the use of films with low permeability to water vapor, would be effective.

4. CONCLUSIONS

Drying of mango occurs during the falling rate period, in two stages independent of airflow used. Fick´s second law can be used to fit experimental drying data and to predict mango behavior inside the evaluated operation range. There is a greater diffusion with increase in temperature and a minor effective diffusion coefficient when velocity airflow diminishes. The effective diffusion coefficient decreased linearly with moisture content and this variation was higher at higher temperatures.

The water diffusion coefficient was higher at increasing temperatures. The Arrhenius equation represented the effective diffusion coefficient variation with temperature. Diffusion prevails during the mango rehydration process, regardless of the addition of solute to the rehydrating solution; therefore, Fick's second law adequately fits the experimental data.

The effective diffusion coefficient is higher for rehydration carried out in sucrose solutions than in glucose solutions. In both cases, the coefficient is greater than the effective coefficient obtained during rehydration in water. Solute addition to the rehydrating solution has a positive effect on water diffusion. The presence of solute produces less weight gain and less water gain in dehydrated samples, but it counteracts the effect of the loss of solids during the rehydration of mangoes in pure water. The initial water contents of the samples are not achieved by any system. The water absorption capacity decreases with solute incorporation.

The rehydration rate decreases linearly with the water content. The water incorporation rate results were higher in glucose-rehydrated samples than in sucrose-rehydrated samples with a decreasing water absorption capacity. There is a high retention of solids in the glucose system.

It is advisable to rehydrate dried mango in a glucose solution for 100 minutes to counteract the effect of the loss of solids on pure water rehydration and to achieve greater water incorporation.

Mango sorption isotherms are of the J type, which is characteristic of foods with high sugar contents. The hysteresis effect is not significant at 25°C or 35°C, but it is clear at 8°C. Isotherms cross over aw = 0.9 for adsorption, due to the higher solubility of sugars. The adsorption surface area decreases when the temperature increases from 8°C to 25°C. The desorption area diminishes as the temperature increases from 8°C to 25°C. A high superficial area is observed during desorption at 35°C. The GAB equation adequately fits the sorption experimental data.

The sorption heat exponentially decreases with increasing moisture and tends toward the pure water value, indicating that the water is freer and more available as the water content increases. The sorption heat value is 10.492 kJ/mol, for water content near the monolayer level of moisture.

REFERENCES

[1] Acevedo, N.C., Briones, V., Buera, P., Aguilera, J.M. 2008. Microstructure affects the rate of chemical, physical and color changes during storage of dried apple discs *Jr of Food Engineering* 85; 222-231.

[2] Akpinar, E.K.; Midelli, A.; Bicer, Y. 2006. The first and second law analyses of thermodynamic of pumpkin drying process. *Jr of Food Engineering* 2006, 72, 320-331.

[3] Al-Mahasneh, M.A., Rababah, T.M., Yang, W. 2007. Moisture sorption thermodynamics of defatted sesame meal (DSM). *Jr of Food Engineering* 81; 735–740.

[4] Al-Muhtaseb, A.H., McMinn, W.A.M., Magee, T.R.A.. 2004. Water sorption isotherms of starch powders. Part 2: Thermodynamic characteristics. *Jr of Food Engineering* 62; 135–142.

[5] Arslan, N Toğrul H. 2006. The fitting of various models to water sorption isotherms of tea stored in a chamber under controlled temperature and humidity. *Jr of Stored Products Research* 42(2); 112-135.

[6] Atarés, L.; Chiralt, A.; González-Martínez, C. 2008. Effect of solute on osmotic dehydration and rehydration of vacuum impregnated apple cylinders (cv. Granny Smith). *Jr of Food Engineering* 89; 49–56.

[7] Aviara, N.A., Ajibola, O.O. 2002. Thermodynamics of moisture sorption in melon seed and cassava. *Jr of Food Engineering* 55; 107 – 113.

[8] Babalis, S.J., Papanicolaou, E., Kyriakis, N., Belessiotis, V.G. 2006. Evaluation of thin-layer drying models for describing drying kinetics of figs (Ficus carica). *Jr of Food Engineering* 75; 205-214.

[9] Baini, R.; Langrish, T.A.G. 2008. An assessment of the mechanisms for diffusion in the drying of bananas. *Jr of Food Engineering* 85; 201–214.

[10] Ben Haj Said, L.; Bellagha, S.; Allaf, K. 2015. Measurements of texture, sorption isotherms and drying/rehydration kinetics of dehydrofrozen-textured apple. *Jr of Food Engineering* 165; 22–33.

[11] Beristain, C. I., García H. S. Azuara, E. 1996. Enthalpy – Entropy Compensation in Food Vapor Adsorption. *Jr of Food Engineering* 30; 405 – 415.

[12] Biju Cletus, A., Carson, J. K. 2008. Drying curves and apparent diffusivity of New Zealand chestnut variety ‘1015’. *Jr of Food Engineering* 85; 381–386.

[13] Bilbao-Sáinz, C. Andrés, A. Fito, P. 2005. Hydration kinetics of dried apple as affected by drying conditions, *Jr of Food Engineering* 68; 369-376.

[14] Brunauer, S., Emmett, P.H., Teller, E. 1938. Adsorption of gases in multimolecular layer. Journal of the American Chemical Society 68; 309-319.

[15] Cassini, A.S., Marczak, L.D.F., Noreña, C.P.Z. 2009. Comparison between the isotherms of two commercial types of textured soy protein. *Latin Amercian Applied Research* 39(2); 91-97.

[16] Cervenka, L., Rezkova, S., Kralovsky, J. 2008. Moisture adsorption characteristics of gingerbread, a traditional bakery product in Pardubice, Czech Republic. *Jr of Food Engineering* 84; 601–607.

[17] Chirife, J., Resnik, S.L. Fontan, C.F. 1985. Application of Ross' equation for prediction of water activity in intermediate moisture food systems. *International Journal of Food Science and Technology* 20; 773-770.

[18] Colato, A.G., Gomes Alves, D., Moreira Azoubel, P. 2008. Effect of processing conditions on the water absorption and texture kinetics of potato. *Jr of Food Engineering* 84; 214–223.

[19] Corzo, O., Bracho, N., Alvarez, C. 2008. Water effective diffusion coefficient of mango slices at different maturity stages during air drying. *Jr of Food Engineering* 87; 479–484.

[20] Corzo, O.; Bracho, N.; Vásquez, A.; Pereira, A. 2008. Optimization of a thin layer drying process for coroba slices. *Jr of Food Engineering* 85; 372–380.

[21] Crank, J. 1975. *The Mathematics of Diffusion*, 2nd Ed. Oxford University Press. London.

[22] Cunningham, S.E., Mcminn, W.A.M., Magee, T.R.A., Richardson, P.S. 2008. Effect of processing conditions on the water absorption and texture kinetics of potato. *Jr of Food Engineering* 84; 214–223.

[23] Dandamrongrak, R., Young, G., Mason, R. 2002. Evaluation of various pre-treatments for the dehydration of banana and selection of suitable drying models. *Jr of Food Engineering* 55; 139–146.

[24] Desmorieux, H., Diallo, C., Coulibaly, Y. 2008. Operation simulation of a convective and semi-industrial mango dryer. *Jr of Food Engineering* 89; 119–127.

[25] Doymaz, İ. 2012. Evaluation of some thin-layer drying models of persimmon slices (Diospyros kaki L.) *Energy Conversion and Management* 56, 199–205.

[26] Falade, K.O., Adedeji, A.A., Akingbala, J.O. 2003. Effect of soybean substitution for cowpea on physical, compositional, sensory and sorption properties of okara Ogbomosho. *European Food Research and Technology* 217(6); 492-497.

[27] Falade, K.O., Aworh, O.C. 2004. Adsorption isotherms of osmo-oven dried african star apple (Chrysophyllum albidum) and african mango (Irvingia gabonensis) slices. *European Food Research and Technology* 218(3); 278-283.

[28] Farahnaky, A.; Kamali, E. 2015. Texture hysteresis of pistachio kernels on drying and rehydration. *Jr of Food Engineering* 166; 335–341.

[29] Fernando,W.J.N.; Ahmad, A.L.; Othman, M.R. . 2011. Convective drying rates of thermally blanched slices of potato (Solamum tuberosum): Parameters for the estimation of drying rates. *Food and Bioproducts Processing* 89(4); 514–519.

[30] Figiel, A. 2010. Drying kinetics and quality of beetroots dehydrated by combination of convective and vacuum-microwave methods. *Jr of Food Engineering* 98; 461–470.

[31] Fontan, C.F., Chirife, J., Sancho, E., Iglesias, H.A. 1982. Analysis of a Model for Water Sorption Phenomena in Foods. *Jr of Food Science* 47(5); 1590-1594

[32] Garau, M.C.; Simal, S.; Femenia, A., Roselló, C. 2006. Drying of orange skin: drying kinetics modelling and functional properties. *Jr of Food Engineering* 75, 288-295.

[33] García-Alvarado, M.A., Salgado-Cervantes, M.A., Rodríguez-Jimenez, G.C., Tejero-Andrade, J.M. Rosado-Zarrabal, T.L. 2002. Detremination of water sorption isosteric heat in papaya (carica papaya) by termal análisis. *Annual Meeting and Food Expo*, Anaheim, California.

[34] García-Pascual, P., Sanjuán, N., Bon, J., Carreres, J., Mulet, A. 2005. Rehydration process of Boletus edulis mushroom: characteristics and modelling. *Jr of the Science of Food and Agriculture* 85; 1397–1404.

[35] García-Pascual, P., Sanjuán, N., Melis, R., Mulet, R. 2006. Morchella esculenta (morel) rehydration process modelling. Journal of Food Engineering 72 (4); 346 – 353.

[36] Giraldo, G., Talens, P., Fito, P., Chiralt, A. 2003. Influence of sucrose solution concentration on kinetics and yield during osmotic dehydration of mango. *Jr of Food Engineering* 58; 33–43.

[37] Giraldo, G., Vázquez, R., Martín-Esparza, M.E., Chiralt, A. 2006. Rehydration kinetics and soluble solids lixiviation of candied mango fruit as affected by sucrose concentration. Journal of Food Engineering 77; 825-834.

[38] González-Fésler, M., Salvatori, D., Gómez, P., Alzamora, S.M. 2008. Convective air drying of apples as affected by blanching and calcium impregnation. *Jr of Food Engineering* 87; 323–332.

[39] Goula, A.M., Karapantsios, T.D., Achilias, D.S., Adamopoulus, K.G. 2008. Water sorption isotherms and glass transition temperature of spray dried tomato pulp. *Jr of Food Engineering* 85; 73–83.

[40] Hubinger, M., Menegalli, F.C., Aguerre, R.J., Suarez, C. 1992. Water vapor adsorption isotherms of guava, mango and pineapple. *Jr of Food Science* 57(6); 1405-1407.

[41] Iglesias, H A., Chirife, J. 1976. Prediction of the effect of temperature on water sorption isotherms of food material. *Jr Food Technology* 11; 109 – 116.

[42] Iglesias, H. A., Chirife, J. Lombardi, J. L. 1975. Water sorption isotherms in sugar beet. *Jr of Food Technology* 10; 299-308.

[43] Iguedjtal, T., Louka N., Allaf K. 2008. Sorption isotherms of potato slices dried and texturized by controlled sudden decompression. *Jr of Food Engineering* 85; 180–190.

[44] Jamradloedluk, J., Nathakaranakule, A. Soponronnarit, S., Prachayawarakorn, S. 2007. Influences of drying medium and temperature on drying kinetics and quality attributes of durian chip. *Jr of Food Engineering* 78; 198–205

[45] Kaptso, K.G., Njintang, Y.N., Komnek. A.E., Hounhouigan, J., Scher, J., Mbofung, C.M.F. 2008. Physical properties and rehydration kinetics of two varieties of cowpea (Vigna unguiculata) and bambara groundnuts (Voandzeia subterranea) seeds. *Jr of Food Engineering* 86; 91–99.

[46] Kaya, A.; Aydın, O.; Dincer, I. 2008. Experimental and numerical investigation of heat and mass transfer during drying of Hayward kiwi fruits (Actinidia Deliciosa Planch) Journal of Food Engineering 88; 323–330.

[47] Kaya, K., Kahyaoglu, T. 2007. Moisture sorption and thermodynamic properties of safflower petals and tarragon. *Jr of Food Engineering* 78; 413–421.

[48] Kaymak-Ertekin, F. 2002. Drying and rehydration kinetics of green and red peppers. *Jr of Food Science* 67; 168–175.

[49] Kaymak-Ertekin, F., Sultanoğlu, M. 2001. Moisture sorption isotherms characteristics of pepper. *Jr of Food Engineering* 47; 225-231.

[50] Kolawole, O., Falade, A., Emmanuel, S., Abbo, B. 2007. Air-drying and rehydration characteristics of date palm (Phoenix dactylifera L.) fruits. *Jr of Food Engineering* 79; 724–730.

[51] Krokida, M.K. Marinos-Kouris, D. 2003. Rehydration kinetics of dehydrated products. *Jr of Food Engineering* 57; 1-7.

[52] Kumar, A.J., Singh, R.R.B., Patil, G.R., Patel, A.A. 2005. Effect of temperature on moisture desorption isotherms of kheer. *Lebensmittel- Wissenschaft und Technologie* 38; 303–310.

[53] Labuza, T.P. Nutrient losses during drying and storage of dehydrated foods. CRC *Critical Reviews in Food Technology* 1972, 9, 217–240.

[54] Labuza, T.P., Kaanane, A., Chen, J.Y. 1985. Effect of temperature on the moisture sorption isotherms and water activity shift of two dehydrated foods. *Jr of Food Science* 50; 385-391.

[55] Lee, K. T., Farid, M., Nguang, S. K. 2006. The mathematical modelling of the rehydration characteristics of fruits. *Jr of Food Engineering* 72, 16 – 23.

[56] Lewicki, P.P. 1998. Effect of pre-drying treatment, drying and rehydration on plant tissue properties: a review. *Jr Food Properties* 1(1); 1-22.

[57] Lewicki, P.P., Pawlak, G. 2003. Effect of Drying on Microstructure of Plant Tissue. *Drying Technology* 21(4); 657–683.

[58] López-Malo, A., Palou, E. Welti, J., Corte, P., Argaiz, A. 1997. Moisture sorption characteristics of blanched and osmotically treated apples and papayas. *Drying Technollogy* 15 (3-4); 1173-1985.

[59] Maldonado, S., Arnau, E., Bertuzzi, A. 2010. Effect of temperature and pretreatment on water diffusion during rehydration of dehydrated mangoes. *Jr of Food Engineering* 96; 333–341.

[60] Marabi, A., Thieme, U., Jacobson, M., Saguy, I.S. 2006. Influence of drying method and rehydration time on sensory evaluation of rehydrated carrots particulates. *Jr of Food Engineering* 72; 211-217.

[61] Marin, B.E., Lemus, M.R., Flores, M.V. 2006. La Rehidratación de Alimentos Deshidratados. *Rev. Chilena de nutrición* 33 (3); 527-538.

[62] Maroulis, Z. B., Tsami, E., Marinos-Kouris, D. 1983. Application of the GAB model to the moisure sorption isotherms for dried fruits. *Jr of Food Engineering* 7; 63-78.

[63] Maroulis, Z.B., Tsami, E., Marinos-Kouris, D., Saravacos D. 1988. Application of the GAB model to the moisture sorption isotherms for dried fruits. *Jr of Food Engineering* 7(1); 63-78.

[64] Marques, L.G.; Prado, M.M.; Freire J. T. 2009. Rehydration characteristics of freeze-dried tropical fruits. *LWT - Food Science and Technology* 42(7); 1232–1237

[65] Martinez Navarrete, N.; Grau Andrés, A. M.; Chiralt Boix, A.; Fito Maupoey, P. 1998. Isotermas de Sorción. En: Termodinámica y Cinética de Sistemas Alimento Entorno. ISBN 84.7721-703-3. *Publicaciones de la Universidad Politécnica de Valencia*.

[66] Maskan, M. 2001. Drying, shrinkage and rehydration characteristics of kiwifruits during hot air and microwave drying. *Jr of Food Engineering* 48; 177 – 182.

[67] Mohamad, A. Mir, M.A., Nirankar N. 1995. Sorption isotherms of fortified mango bars Journal of Food Engineering 25(1); 141-150.

[68] Moreira, R., Chenlo, F., Chaguri, L., Fernandes, C. 2008a. Water absorption, texture, and color kinetics of air-dried chestnuts during rehydration. *Jr of Food Engineering* 86; 584–594.

[69] Moreira, R., Chenlo, F., Torres, M.D., Vallejo, N. 2008b. Thermodynamic analysis of experimental sorption isotherms of loquat and quince fruits. Journal of Food Engineering 88; 514–521.

[70] Nieto, A.; Castro, M.A.; Alzamora, S.M. 2001. Kinetics of moisture transfer during air drying of blanched and/or osmotically dehydrated mango. *Jr of Food Engineering* 50; 175–185.

[71] Orikasa T.; Wub, L.; Takeo Shiina, A.; Akio Tagawa, C. 2008. Drying characteristics of kiwifruit during hot air drying. *Jr of Food Engineering* 85; 303–308.

[72] Pani, P.; Avitabile Leva, A.; Riva, M.; Maestrelli, A.; Torreggiani, D. 2008. Influence of an osmotic pre-treatment on structure-property relationships of air-dehydrated tomato slices. *Jr of Food Engineering* 86; 105–112.

[73] Pereira da Silva, W.; Pereira da Silva e Silva, C.M.D., Farias Aires, J.E.; Freire da Silva, J. 2014. Osmotic dehydration and convective drying of coconut slices: Experimental determination and description using one-dimensional diffusion model. *Jr of the Saudi Society of Agricultural Sciences.* 13(2), June 2014; 162–168

[74] Pérez-Alonso C., Beristain C., Lobato-Calleros C. 2006 Thermodynamic analysis of the sorption isotherms of pure and blended carbohydrate polymers. *Jr of Food Engineering* 77(4) 753-760

[75] Prachayawarakorn, S., Tia, W., Plyto, N., Soponronnarit, S. 2008. Drying kinetics and quality attributes of low-fat banana slices dried at high temperature. *Jr of Food Engineering* 85; 509–517.

[76] Roberts, J.S.; Tong, C.H. 2003. The development of an isothermal drying apparatus and the evaluation of the diffusion model on hygroscopic porous material. International *Jr of Food Properties* 6(1); 165–180.

[77] Saguy, S. I., Marabi, A., Wallach, R. 2005a. New approach to model rehydration of dry food particulates utilizing principles of liquid transport in porous media. *Trends in Food Science&Technology* 16; 495-506.

[78] Saguy, S.I., Marabi A., Wallach R. 2005b. Liquid imbibition during rehydration of dry porous foods. *Innovative Food Science & Emerging Technologies* 6(1); 37-43

[79] Sanjuán N., Bon J., Clemente G., Mulet A. 2004. Changes in the quality of dehydrated broccoli florets during storage. *Jr of Food Engineering* 62(1); 15-21.

[80] Sanjuán, N., Andrés, J. Clemente, G. Mulet, A. 2001. Modeling of the rehydration process of broccoli florets, Eur. *Food Ressearch Technology* 212; 449.

[81] Saravacos, D. A., Tsiourvas, D. A., Tsami, E. 1986. Effect of temperature on the water adsorption isotherms of sultana raisins. *Jr of Food Science* 51(2); 381-387.

[82] Seremet, L.; Botez, E.; Nistor, O.V.; Andronoiu, D. G.; Mocanu, G.D. 2015. Effect of different drying methods on moisture ratio and rehydration of pumpkin slices. *Food Chemistry*. doi:10.1016/j.foodchem.2015.03.125.

[83] Simal, S.; Femenia, A.; Garau, M.C.; Roselló, C. 2005. Use of exponential, Page´s and diffusional models to simulate the drying kinetics of kiwi fruit. *Jr of Food Engineering* 66; 323-328.

[84] Singh, G.D.; Sharma, R.; Bawa, A.S.; Saxena, D.C. 2008. Drying and rehydration characteristics of water chestnut (Trapa natans) as a function of drying air temperature. *Jr of Food Engineering* 87; 213–221.

[85] Sinija, V.R., Mishra, H.N. 2008. Moisture sorption isotherms and heat of sorption of instant (soluble) green tea powder and green tea granules. *Jr of Food Engineering* 86(4); 494-500.

[86] Sun, L.M., Meunier, F. 1987. A Detailed Model for Nonisothermal Sorption in Porous Adsorbents. *Chemical Engineering Science* 42; 1585-1593.

[87] Thuwapanichayanan, R., Prachayawarakorn, S., Soponronnarit, S. 2008. Drying characteristics and quality of banana foam mat. *Jr of Food Engineering* 86; 573–583.

[88] Toğrul, I.T., Pehlivan, D. 2003. Modelling of drying kinetics of single apricot. *Jr of Food Engineering* 58; 23-32.

[89] Torreggiani, D., Bertolo, G. 2001. Osmotic pre-treatments in fruit processing: chemical, physical and structural effects. *Jr of Food Engineering* 49; 247–253.

[90] Tsami, E., Marinos-Kouris, D., Maroulis, E.B. 1990. Water sorption isotherms of raisins, currants, figs, prunes and apricots. *Jr Food Science* 45(6); 1594-1597.

[91] Tunde-Akintunde, T.Y.; Ogunlakin, G.O. 2011. Influence of drying conditions on the effective moisture diffusivity and energy requirements during the drying of pretreated and untreated pumpkin. *Energy Conversion and Management* 52 (2); 1107–1113.

[92] van der Sman, R.G.M.; Vergeldt, F.J.; Van As, H.; van Dalen, G.; Voda, A.; van Duynhoven, J.P.M. 2014. Multiphysics pore-scale model for the rehydration of porous foods. Innovative Food Science & Emerging Technologies 24; 69–79.

[93] Vazquez, G., Chenlo, F., Moreira, R., Carballo, L. 1999. Desorption isotherms of muscatel and aledo grapes, and the influence of pretreatments on muscatel isotherms *Jr of Food Engineering* 39; 409-414.

[94] Vega-Gálvez, A., Aravena, E.L., Mondaca R.L. 2006. Isotermas de adsorción en harina de maíz (Zea mays L.). *Ciência Tecnologia Alimentos* 26(4); 821-827.

[95] Vega-Gálvez, A., Lemus-Mondaca, R., Bilbao-Sáinz, C, Fito, P., Andrés, A. 2008. Effect of air drying temperature on the quality of rehydrated dried red bell pepper (var. Lamuyo) *Jr of Food Engineering* 85; 42–50.

[96] Vega-Mercado, H., Barbosa-Cánovas, G. 2000. The use of GAB model to represent freeze-dried pineapple *Food Dehydration* 89(297), 114-117.

[97] Velić, D., Planinic, M., Tomas, S., Bilic, M. 2004. Influence of airflow velocity on kinetics of convection apple drying, *Jr of Food Engineering* 64; 97-102.

[98] Vergeldt, F.J.; van Dalen, G.; Duijster, A.J. ; Voda, A. ; Khalloufi, S. ; van Vliet, L.J. ; Van As, H. ; van Duynhoven, J.P.M.; van der Sman, R.G.M. 2014. Rehydration kinetics of freeze-dried carrots. *Innovative Food Science and Emerging Technologies* 24; 40–47.

[99] Viollaz, P. E., Alzamora, S. M. 2000. Food Dehydration. *Encyclopedia of Life Support Systems* (EOLSS). Ed. Gustavo B. Barbosa-Cánovas. EOLSS Publishers Co. Ltd. USA.

[100] Wang, N., Brennan, J. G. 1991. Moisture sorption isotherm characteristics of potatoes at four temperatures. Jr of Food Engineering 14; 269–287.

[101] Wang, Z.; Sun, J.; Liao, X; Chen, F.; Zhao, G.; Wu, J.; Hu, X. 2007. Mathematical modeling on hot air drying of thin layer apple pomace. Food Research International 40; 39–46.

[102] Welti, J., Palou, E., Lopez Malo, A. Balseira, A. 1995. Osmotic concentration. Drying of mango slices. Drying Technology 13(12); 405-416.

[103] Xanthopoulos, G.; Yanniotis, S.; Boudouvis, A.G. 2012. Numerical Simulation of Variable Water Diffusivity during Drying of Peeled and Unpeeled Tomato. Jr of Food Science. 77(10); E287–E296.

[104] Yan, Z., Sousa-Gallagher, M. J., Oliveira, F.A.R. 2008a. Shrinkage and porosity of banana, pineapple and mango slices during air-drying. *Jr of Food Engineering* 84; 430–440.

[105] Yan, Z., Sousa-Gallagher, M. J., Oliveira, F.A.R. 2008b. Sorption isotherms and moisture sorption hysteresis of intermediate moisture content banana. *Jr of Food Engineering* 86; 342–348.